scientific reports

Check for updates

OPEN

A novel pressure control method for nonlinear shell-and-tube steam condenser system via electric eel foraging optimizer

Serdar Ekinci[1], Cebrail Turkeri[1], Davut Izci[2,3], Laith Abualigah[4], Mohit Bajaj[5,6,7]✉, Vojtech Blazek[8] & Lukas Prokop[8]

Precise pressure control in shell-and-tube steam condensers is crucial for ensuring efficiency in thermal power plants. However, traditional controllers (PI, PD, PID) struggle with nonlinearities and external disturbances, while classical tuning methods (Ziegler-Nichols, and Cohen-Coon) fail to provide optimal parameter selection. These challenges lead to slow response, high overshoot, and poor steady-state performance. To address these limitations, this study proposes a cascaded PI-PDN control strategy optimized using the electric eel foraging optimizer (EEFO). EEFO, inspired by the prey-seeking behavior of electric eels, efficiently tunes controller parameters, ensuring improved stability and precision. A comparative analysis against recent metaheuristic algorithms (SMA, GEO, KMA, QIO) demonstrates superior performance of EEFO in regulating condenser pressure. Additionally, validation against documented studies (CSA-based FOPID, RIME-based FOPID, GWO-based PI, GA-based PI) highlights its advantages over existing methods. Simulation results confirm that EEFO reduces settling time by 22.7%, overshoot by 78.7%, steady-state error by three orders of magnitude, and ITAE by 81.2% compared to metaheuristic based methods. The EEFO-based controller achieves faster convergence, enhanced robustness to disturbances, and precise tracking, making it a highly effective solution for real-world applications. These findings contribute to optimization-based control strategies in thermal power plants and open pathways for further bio-inspired control innovations.

Keywords Electric eel foraging optimizer, Pressure control, Nonlinear system, Steam condenser, Cascaded PI-PDN controller, Metaheuristics

Steam condensers are integral components in thermal power plants, tasked with converting exhaust steam from turbines into liquid water, which is then recirculated back into the boiler[1]. This process is essential not only for improving the efficiency of the power generation cycle but also for maintaining the system's operational stability and desired parameters[2]. The effectiveness of a steam condenser directly influences the overall performance, efficiency, and reliability of the power plant[3–5]. Maintaining optimal pressure within the steam condenser is crucial for ensuring efficient operation. Improper pressure control can lead to inefficient condensation, higher energy consumption, and potential damage to the condenser and related equipment[6,7]. Thus, precise pressure regulation is imperative to achieve efficient and stable operation in thermal power plants.

To address the challenges of controlling condenser pressure, various control methodologies have been explored. Adaptive control methods, which dynamically adjust controller parameters based on real-time system behavior, offer significant advantages in managing nonlinearities and time-varying dynamics[8,9]. These methods enhance the system's ability to respond to unforeseen disturbances and changes in operating conditions by continuously updating control parameters to maintain optimal performance. In addition to adaptive strategies, artificial intelligence (AI) based control techniques have gained prominence due to their capability to handle

[1]Department of Computer Engineering, Batman University, Batman 72100, Turkey. [2]Department of Electrical and Electronics Engineering, Bursa Uludag University, Bursa 16059, Turkey. [3]Applied Science Research Center, Applied Science Private University, Amman 11931, Jordan. [4]Computer Science Department, Al Al-Bayt University, Mafraq 25113, Jordan. [5]Department of Electrical Engineering, Graphic Era (Deemed to Be University), Dehradun 248002, India. [6]College of Engineering, University of Business and Technology, Jeddah 21448, Saudi Arabia. [7]Graphic Era Hill University, Dehradun 248002, India. [8]ENET Centre, CEET, VSB-Technical University of Ostrava, Ostrava 708 00, Czech Republic. ✉email: thebestbajaj@gmail.com

complex and nonlinear systems effectively. Approaches utilizing neural networks, fuzzy logic, and expert systems have been successfully applied to condenser pressure control, demonstrating improved adaptability and robustness compared to traditional methods[10]. AI-based controllers can learn and model intricate system behaviors, enabling more precise and efficient control under varying operational scenarios[11].

Robust control strategies, such as PI, PD, PID, and PDN controllers, are widely used due to their simplicity and effectiveness in maintaining system performance under diverse conditions and disturbances[12]. These controllers have been extensively studied and applied in thermal power plants, where they help stabilize operations despite the challenges posed by fluctuating load demands and environmental factors. Among these, cascaded control structures, such as the PI-PDN controller, have shown superior performance in managing complex and highly nonlinear systems like steam condensers. The cascaded configuration combines the strengths of both controllers, where the PI controller manages the primary control loop by handling steady-state errors, and the PDN controller addresses the secondary loop by improving transient response and mitigating the effects of measurement noise. This hierarchical control structure enhances overall system stability, response speed, disturbance rejection capabilities and noise attenuation. However, the effectiveness of cascaded controllers like PI-PDN heavily depends on the accurate tuning of their parameters. Determining the optimal values for the proportional gain (K_p), integral gain (K_i), derivative gain (K_d), and filter coefficients is a complex task that significantly influences the controller's performance[13]. Improper tuning can lead to issues such as overshoot, prolonged settling times, and instability, undermining the benefits offered by the cascaded control structure.

Traditional tuning methods, such as the Ziegler-Nichols and Cohen-Coon approaches, provide heuristic rules for parameter selection but often fall short in delivering optimal performance, especially in systems with complex and nonlinear dynamics[14,15]. For instance, the Ziegler-Nichols method, while simple and easy to implement, can result in aggressive tuning that leads to oscillatory responses. Similarly, the Cohen-Coon method, though more conservative, is tailored for first-order systems with dead time and may not suit all applications[16]. These conventional methods are generally inadequate for finely tuning multiple parameters in cascaded controllers, as they do not effectively account for the intricate interactions between different control loops and the system's nonlinear behavior.

Given the limitations of classical tuning techniques, modern optimization algorithms have gained traction for their ability to fine-tune controller parameters more effectively. Techniques such as genetic algorithm (GA), particle swarm optimization (PSO), and differential evolution (DE) have been applied to optimize PI or cascaded controller parameters, demonstrating significant improvements in control accuracy and system stability[17]. These advanced methods employ stochastic search mechanisms and exploit evolutionary principles to explore the solution space thoroughly, identifying optimal or near-optimal parameter sets that enhance controller performance under various operating conditions. Among these modern optimizers, sparrow search algorithm (SSA)[18], the slime mould algorithm (SMA)[19], golden eagle optimizer (GEO)[20], komodo mlipir algorithm (KMA)[21], quadratic interpolation optimization (QIO)[22], chaotic quasi-oppositional arithmetic optimization algorithm (COAOA)[23], cuckoo optimization algorithm (COA)[24]have shown considerable promise in various engineering applications. These algorithms offer unique strengths, such as efficient exploration of the search space and robust convergence characteristics, making them suitable for optimizing complex control systems. For example, SMA uses the behavior of slime mould in nature to balance exploration and exploitation during the search process, while GEO simulates the hunting behavior of golden eagles to guide the search towards optimal solutions. Similarly, KMA is inspired by the unique movement of komodo dragons and QIO leverages quadratic interpolation techniques to enhance search capabilities. In addition to this, the electric eel foraging optimizer (EEFO) stands out as a promising method due to its unique approach to exploring and exploiting the search space. The algorithm models the hunting strategy of electric eels, which generate electric fields to detect and capture prey, and applies this strategy to navigate optimization landscapes. The EEFO method has been successfully applied to a range of optimization problems, including parameter extraction in photovoltaic systems[25,26]and control schemes for temperature adjustment in electric furnaces[27].

In this proposed study, the EEFO, a novel bio-inspired algorithm, to optimize the parameters of a cascaded PI-PDN controller for a nonlinear shell-and-tube steam condenser system is introduced. This study marks the first application of EEFO for pressure control in a nonlinear shell-and-tube steam condenser system. The EEFO algorithm is inspired by the foraging behavior of electric eels, which generate electric fields to locate prey, effectively navigating and exploiting the search space in optimization problems[28]. By applying EEFO to the task of condenser pressure control, it is aimed to demonstrate its superior performance compared to existing optimization techniques.

The novelty and key contributions of this study are as follows:

1. First-ever application of EEFO for cascaded PI-PDN controller tuning in nonlinear condenser pressure control – While EEFO has been previously explored in other optimization problems, this study introduces its first application to pressure regulation in shell-and-tube steam condensers, demonstrating its effectiveness in handling nonlinearities and disturbances.
2. Superior performance over recent metaheuristic algorithms – A detailed comparative analysis against SMA, GEO, KMA, and QIO optimization techniques highlights the higher efficiency of EEFO in reducing settling time, overshoot, steady-state error, and ITAE. EEFO achieves 22.7% faster settling time, 78.7% lower overshoot, and three orders of magnitude lower steady-state error compared to these methods.
3. Significant improvements over documented control strategies – The proposed EEFO-based PI-PDN controller is benchmarked against CSA-based FOPID, RIME-based FOPID, GWO-based PI, and GA-based PI from existing literature, confirming its superiority in terms of stability, response time, and robustness in condenser pressure control.

4. Advancement of bio-inspired optimization in industrial control – By applying EEFO to a complex nonlinear control problem, this study expands the scope of bio-inspired algorithms for industrial automation, particularly in thermal power plant operations, paving the way for further research in bio-inspired control strategies.

The structure of the paper is organized as follows: Sect. 2 discusses the EEFO in depth. Section 3 details the dynamic modeling of the shell-and-tube steam condenser system. Section 4 presents the design of the cascaded PI-PDN controller optimized using EEFO. Section 5 gives the simulation results and compares with other popular meta-heuristic methods. Finally, Sect. 6 concludes the paper with a summary of findings.

EEFO algorithm

The EEFO is a bio-inspired optimization algorithm, rooted in the predatory behavior of electric eels[28–30]. These eels utilize electric fields to detect and capture prey, a behavior that has been translated into a robust search mechanism within the EEFO algorithm. The EEFO algorithm operates by mimicking the sequential behaviors of electric eels, including interaction, resting, hunting, and migration. Each of these behaviors is mathematically modeled to enhance both the exploration and exploitation capabilities of the algorithm, thereby improving its ability to find optimal solutions.

The process begins with the interaction among candidate solutions, which are represented as individual eels within a population. Each candidate solution interacts with others, guided by the best-performing solution, or "prey" within the population. The interaction is mathematically expressed by adjusting the position of each candidate solution based on a stochastic component and the relative position of the best solution. This interaction ensures that the population is drawn towards promising areas in the search space. During the interaction, the position update of each candidate solution is governed by the following equation[27]:

$$v_i\left(t+1\right) = x_j\left(t\right) + n_1 \cdot \left(\bar{x}\left(t\right) - x_i\left(t\right)\right) \tag{1}$$

where n_1 is a random number following a normal distribution, $\bar{x}\left(t\right)$ represents the mean position of the population and $x_j\left(t\right)$ is the position of a randomly selected candidate solution. This equation helps each candidate refine its position based on the collective behavior of the population.

Following the interaction phase, the algorithm simulates a resting period, where candidate solutions temporarily cease movement to conserve energy. This phase is crucial for preventing premature convergence by allowing the algorithm to pause and explore alternative directions. The resting behavior is modeled by adjusting the positions of candidate solutions with an additional random component, which introduces variability and maintains diversity within the population. Mathematically, this resting behavior is described by[27]:

$$v_i\left(t+1\right) = R_i\left(t+1\right) + n_2 \cdot \left(R_i\left(t+1\right) - round\left(rand\right) \cdot x_i\left(t\right)\right) \tag{2}$$

where $R_i\left(t+1\right)$ represents the resting position, and n_2 is another normally distributed random variable. This ensures that the candidate solutions do not stagnate but continue to explore the search space in a controlled manner.

As the algorithm progresses, it enters the hunting phase, where the candidate solutions intensify their search around the best solutions, simulating the eel's behavior when it encircles its prey. This phase enhances the algorithm's exploitation ability, focusing on fine-tuning the solutions by narrowing the search around areas of high potential. The position update during this phase is defined in Eq. (3)[27].

$$v_i\left(t+1\right) = H_{prey}\left(t+1\right) + \eta \cdot \left(H_{prey}\left(t+1\right) - round\left(rand\right) \cdot x_i\left(t\right)\right) \tag{3}$$

where $H_{prey}\left(t+1\right)$ denotes the updated position of the prey and η is a factor that controls the intensity of the hunting behavior.

Finally, the migration behavior is introduced to balance exploration and exploitation by allowing candidate solutions to move from their resting positions to more promising areas. This migration is critical for avoiding local optima and ensuring that the search space is thoroughly explored. The position update during this migration phase is modeled in Eq. (4)[27].

$$v_i\left(t+1\right) = -r_5 \cdot R_i\left(t+1\right) + r_6 \cdot \left(H_r\left(t+1\right) - L \cdot \left(H_r\left(t+1\right) - x_i\left(t\right)\right)\right) \tag{4}$$

where $H_r\left(t+1\right)$ represents a target position in the hunting area, r_5 and r_6 are random variables and L is a Levy flight function that enhances the exploration of the search space. Throughout these phases, the algorithm dynamically adjusts the balance between exploration and exploitation using an energy factor $E\left(t\right)$, which determines the focus of the search process. The energy factor is calculated in Eq. (5)[27].

$$E\left(t\right) = 4 \cdot \sin\left(1 - \frac{t}{T}\right) \cdot \ln\left(\frac{1}{r_7}\right) \tag{5}$$

where r_7 is a random number, and T is the maximum number of iterations. The application of the EEFO algorithm in optimizing control parameters for a cascaded PI-PDN controller in a nonlinear shell-and-tube steam condenser system demonstrates its effectiveness. By optimizing parameters such as proportional gain, integral gain, derivative gain, and filter coefficients, the EEFO algorithm enhances system stability, reduces

response time, and improves robustness against disturbances. The mathematical constructs behind EEFO, coupled with its bio-inspired approach, make it a powerful tool for solving complex optimization problems in dynamic environments.

Modeling of shell-and-tube steam condenser

Shell-and-tube steam condensers play a vital role in thermal power plants by condensing exhaust steam from turbines into liquid water, which can then be recycled within the system[31]. This process not only enhances the efficiency of the power plant but also maintains the desired pressure levels within the condenser. The condenser typically consists of a cylindrical shell enclosing a bundle of tubes. Steam flows through the shell side, where it comes into contact with the cooler water flowing inside the tubes, facilitating effective heat exchange[8]. Figure 1 illustrates the typical schematic diagram of shell-and-tube steam, highlighting the flow paths of steam and cooling water.

3.1 Mathematical model of the condenser

To comprehensively model the dynamic behavior of the shell-and-tube steam condenser, both the heat transfer and fluid flow processes must be considered[8]. The primary function of the condenser is to transfer heat from the steam to the cooling water, enabling the condensation of steam into liquid condensate. This heat transfer process can be quantified using the overall heat transfer equation[12]:

$$Q = U \cdot A \cdot \Delta T_m \tag{6}$$

where Q is the rate of heat transfer, U is the overall heat transfer coefficient, A is the heat transfer area and ΔT_m is the logarithmic mean temperature difference. The logarithmic mean temperature difference (ΔT_m) is calculated in Eq. (7)[12].

$$\Delta T_m = \frac{(T - T_{cw})}{\ln\left(\frac{T_c - T_{cw}}{T_c - T}\right)} \tag{7}$$

where T_{cw}, T_c and T are the inlet temperature of the cooling water, condensate temperature and outlet temperature of the cooling water, respectively. The energy balance equations for the steam (shell side) and cooling water (tube side) is expressed in Eq. (8)[12].

$$Q = F_c \cdot \lambda \tag{8}$$

where F_c is the mass flow rate of the steam and λ is the specific latent heat of vaporization. Cooling water side energy balance is as follows[12]:

$$\frac{dT}{dt} = \frac{F_{cw}}{M_{cw}}(T_{cw} - T) + \frac{Q}{M_{cw} \cdot C_P} \tag{9}$$

where F_{cw} is the mass flow rate of cooling water, M_{cw} is the cooling water holdup, C_P is the specific heat capacity of cooling water. Using the Wilson Plot method, the product of the overall heat transfer coefficient and the heat transfer area ($U \cdot A$) can be approximated by Eq. (10)[12].

$$\frac{1}{U \cdot A} = a_1 \cdot F_{cw}^{-0.8} + a_2 \tag{10}$$

where a_1 and a_2 are constants. The mass balance for both steam and condensate assumes that their volumes remain constant, implying that the condensate's outlet flow rate is regulated to keep a steady condensate level

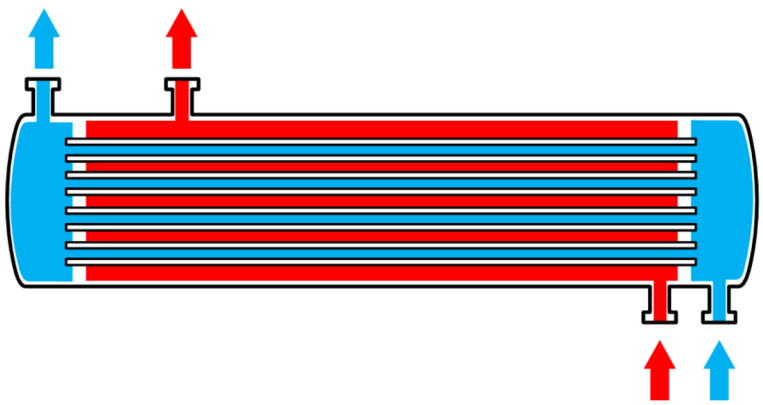


Fig. 1. Schematic diagram of shell-and-tube steam condenser.

Parameter	Value	Unit
R	0.461526	kJ/(kgK)
V	3	m^3
λ	2265.65	kJ/kg
$U \cdot A$	356.972	kW/K
M_{cw}	6500	kg
C_P	4.2	kJ/(kgK)
α	0.3162	K/kPa
β	68.0958	°C
α_1	0.087292	-
α_2	0.00073787	-

Table 1. Condenser parameters.

Parameter	Value	Unit	Description
F_a	4	kg/s	Steam flow rate
F_c	4	kg/s	Condensate flow rate
F_{cw}	107.8881	kg/s	Cooling water flow rate
P	90	kPa	Condenser pressure
T	80	°C	Cooling water outlet temperature
T_{cw}	60	°C	Cooling water inlet temperature
T_c	96.5538	°C	Condensate temperature
Q	9062.6	kW	Heat duty

Table 2. Condenser variables.

within the condenser. The dynamic equation governing the pressure within the condenser is expressed in Eq. (11)[12].

$$\frac{dP}{dt} = \frac{RT_c}{V}(F_s - F_c) \tag{11}$$

where P represents the condenser pressure, R is the specific gas constant, V is the condenser volume, and F_s is the mass flow rate of steam. The relationship between the condensate temperature T_c and the pressure P is linearly approximated in Eq. (12)[12].

$$T_c = \alpha P + \beta \tag{12}$$

where α and β are coefficients determined based on system specifications. The dynamic behavior of the shell-and-tube steam condenser is captured by integrating the energy balances and pressure dynamics equations. The energy transfer between the steam and cooling water is governed by the heat transfer rate Q, which is determined by both the overall heat transfer coefficient $U \cdot A$ and the latent heat of vaporization λ. By solving the coupled differential Eqs. (9) and (11) alongside the empirical relation (10), the model can predict the transient response of the condenser's temperature and pressure under varying operational conditions. This comprehensive mathematical framework allows for the simulation and optimization of the condenser's performance, providing essential insights for the design and control of the system. The parameters and variables outlined in Tables 1 and 2 are essential for accurately modeling the condenser's behavior.

Proposed novel cascaded control method

The proposed control method utilizes a cascaded PI-PDN controller to regulate the pressure within a nonlinear shell-and-tube steam condenser system. The cascaded structure combines the strengths of the PI and PDN controllers and block diagram of the cascaded PI-PDN controller is illustrated in Fig. 2. This configuration enhances the system's ability to handle both steady-state errors and transient responses, making it particularly effective for controlling complex, nonlinear systems such as steam condensers.

The cascaded PI-PDN controller is designed to manage two critical aspects of control: steady-state accuracy and transient response. The primary loop is governed by the PI controller, which addresses the steady-state error by integrating the error signal over time. The secondary loop is managed by the PDN controller, which improves the system's transient response and mitigates the effects of measurement noise. The PI controller's output is defined in Eq. (13)[32].

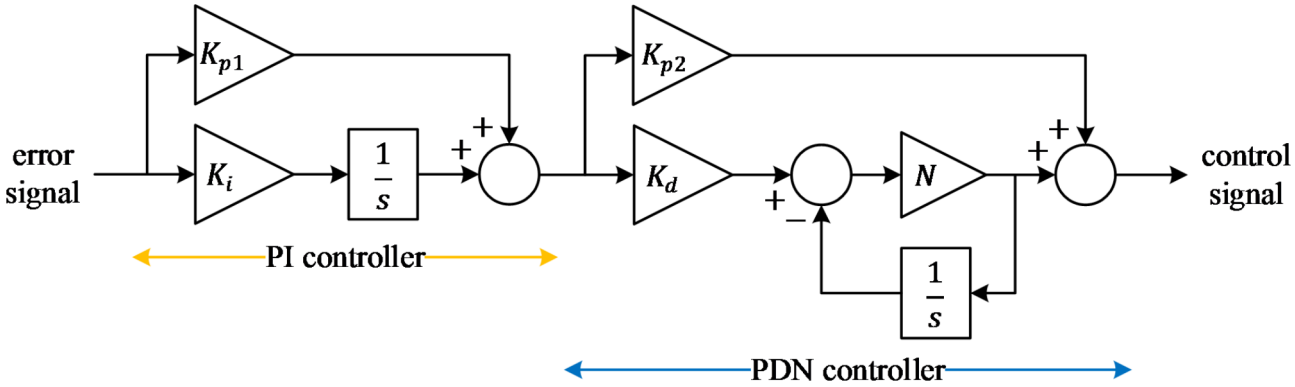


Fig. 2. Block diagram of cascaded PI-PDN controller.

$$u_1(t) = K_{p1} \cdot e(t) + K_i \cdot \int_0^t e(t)\, dt \tag{13}$$

where $u_1(t)$ is the control signal from the PI controller, K_{p1} is the proportional gain of the PI controller, K_i is the integral gain and $e(t)$ is the error signal at time t. The PDN controller's output, which forms the secondary control loop, is expressed in Eq. (14)[33].

$$u_2(t) = K_{p2} \cdot u_1(t) + K_d \cdot \frac{du_1(t)}{dt} + \left(-\frac{1}{N} \cdot \frac{du_2(t)}{dt}\right) \tag{14}$$

In the cascaded configuration, the output of the PI controller $u_1(t)$ is fed as the input to the PDN controller. This structure allows the PI controller to address the slower dynamics related to steady-state performance, while the PDN controller handles the faster dynamics and noise, resulting in a more robust and responsive control system.

To optimize the performance of the cascaded PI-PDN controller, ITAE is used as the objective function. The ITAE criterion emphasizes the minimization of errors that persist over time, making it suitable for evaluating the effectiveness of control systems in dynamic environments. The ITAE objective function is described by Eq. (15)[34].

$$ITAE = \int_{t_{fault}}^{t_{sim}} |e(t)|\,(t - t_{fault})dt \tag{15}$$

where $t_{sim} = 50$ second is the total simulation time and $t_{fault} = 10$ second is the time at which a disturbance (or fault) is introduced. The ITAE criterion was selected as the objective function due to its effectiveness in minimizing long-term error accumulation while prioritizing rapid error reduction. Compared to other traditional integral-based performance indices, ITAE offers distinct advantages in optimizing transient response and disturbance rejection. For example, while integral of absolute error (IAE) minimizes total absolute error, it does not differentiate between early and late errors, which may lead to longer settling times in control applications. The integral of squared error (ISE) penalizes larger deviations more aggressively, making it suitable for systems with high sensitivity to large errors. However, it often compromises response time and may allow prolonged small errors, affecting steady-state accuracy. The integral of time-weighted squared error (ITSE) provides a balance between transient and steady-state errors, but it does not penalize sustained errors as effectively as ITAE, which is crucial for condenser pressure regulation. By assigning greater weight to errors occurring later in the response, ITAE ensures that prolonged deviations are heavily penalized, forcing the controller to achieve faster convergence and minimal steady-state error. As seen in the comparative results, the EEFO-optimized PI-PDN controller tuned using ITAE achieves superior performance in settling time, overshoot reduction, and steady-state precision, confirming its suitability for this nonlinear control problem.

The optimization of the cascaded PI-PDN controller's parameters is subject to predefined boundaries to ensure that the search space is both feasible and efficient showed Table 3. These boundaries are chosen based on the physical characteristics of the steam condenser system and the desired performance criteria. The proposed EEFO-based cascaded PI-PDN controller is applied to the steam condenser system as illustrated in Fig. 3. The process begins with an input step test, where a disturbance is introduced to the system. The error signal, defined as the difference between the desired pressure setpoint and the actual pressure, is fed into the cascaded PI-PDN controller. The controller adjusts the parameters K_{p1}, K_i, K_{p2}, K_d and N based on the feedback from the system and the evaluation of the ITAE value. The EEFO algorithm then determines the behavior of each eel in the population, whether to perform interacting, resting, migrating, or hunting behaviors, based on the energy factor $E(t)$ and random probabilities. These behaviors guide the search for optimal controller parameters, iteratively

Bounds	K_{p1}	K_i	K_{p2}	K_d	N
Lower bound	1	0.1	1	0.05	10
Upper bound	20	10	20	5	500

Table 3. Adopted boundaries of the controller parameters.

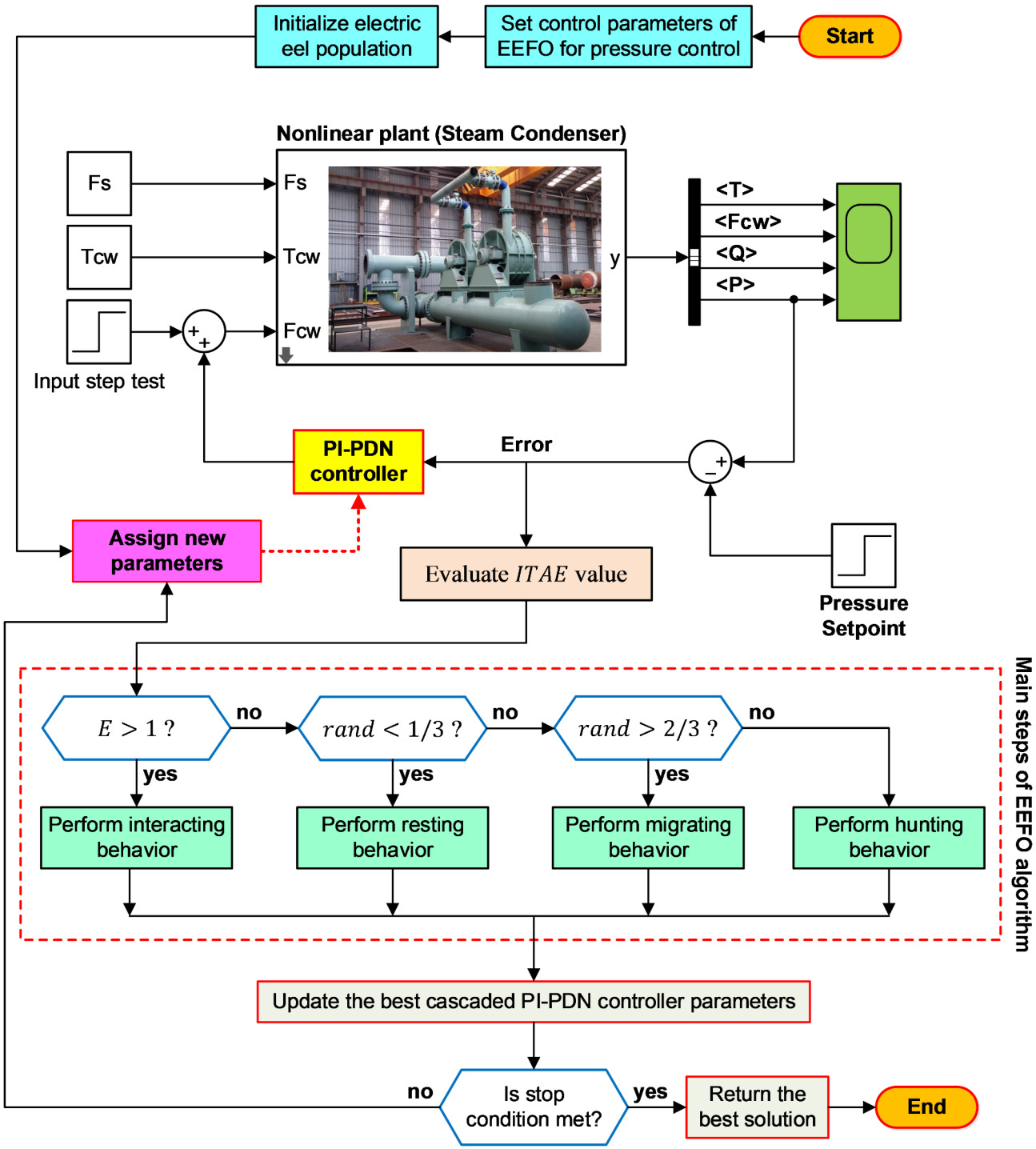


Fig. 3. Application of the proposed EEFO based cascaded PI-PDN controller to steam condenser.

improving the system's performance. The process continues until the stopping criterion is met, at which point the algorithm returns the best solution, corresponding to the optimal set of controller parameters. This solution is then applied to the PI-PDN controller, ensuring that the steam condenser system operates efficiently and maintains stable pressure control under various conditions.

Simulation results

The comprehensive simulation results obtained by applying the proposed EEFO to a cascaded PI-PDN controller for pressure control in a nonlinear shell-and-tube steam condenser system is presented in this section. The performance of the EEFO algorithm is compared with several recent metaheuristic algorithms, and its robustness under various conditions is assessed.

Recent metaheuristic algorithms

The effectiveness of the proposed EEFO algorithm is evaluated by comparing it with four recent metaheuristic algorithms: QIO[22], KMA[21], GEO[20], and SMA[19]. Each algorithm was applied to tune the parameters of the cascaded PI-PDN controller under identical simulation conditions to ensure a fair comparison. The parameters in Table 4. indicate that all algorithms were tested with a consistent population size of 30 and a total of 50 iterations. These settings were selected to balance computational efficiency with optimization performance.

The boxplot analysis presented in Fig. 4 compares the distribution of ITAE values obtained from multiple runs of each algorithm. The EEFO algorithm consistently achieved lower ITAE values with reduced variability compared to the other algorithms. This suggests that EEFO not only finds better solutions but does so more reliably across different runs. The smaller spread in the EEFO boxplot indicates that the algorithm is less sensitive to initial conditions and stochastic variations, which is crucial for practical applications where consistency is key.

A detailed statistical analysis of the ITAE values obtained by each algorithm has been provided in Table 5. The EEFO algorithm outperforms the other methods across several metrics, including achieving the lowest minimum, maximum and average ITAE values. However, in terms of standard deviation, which measures the variability or dispersion of the ITAE values, EEFO does not have the lowest value; QIO, KMA and GEO demonstrate smaller variations with standard deviations of 0.1048, 0.0678 and 0.0726, respectively. Despite this, EEFO's strong performance in minimizing ITAE and its competitive standard deviation underscore its effectiveness and reliability in optimizing control parameters. The lowest Friedman's mean rank of 1 for EEFO indicates its superior performance compared to the other optimizers, highlighting its robustness and reliability. This statistical consistency suggests that EEFO is less likely to result in suboptimal performance in practical applications, making it a highly effective choice for optimizing control parameters.

The convergence curves for the ITAE objective function across different algorithms are presented in Fig. 5. The rapid convergence of EEFO is evident, as it reaches a near-optimal solution faster. This quick convergence is advantageous in real-time applications where computational efficiency is critical. Additionally, EEFO not only converges quickly but also to a lower ITAE value, indicating its effectiveness in exploring the solution space thoroughly and avoiding local minimum.

The controller parameters listed in Table 6 highlight the effectiveness of EEFO in finding balanced and optimal settings for the cascaded PI-PDN controller. The respective table demonstrates the effectiveness of EEFO in optimizing the settings for the cascaded PI-PDN controller. The values obtained through EEFO, particularly for K_{p2}, K_d and the filter coefficient N, suggest a carefully balanced approach that enhances overall system performance. Specifically, EEFO achieved a higher K_d value compared to the other algorithms, which can help in improving the system's responsiveness to changes, reducing the impact of oscillations, and effectively filtering noise. Additionally, the relatively moderate filter coefficient N in EEFO, compared to those in KMA, GEO and

Algorithm	Parameter	Value
EEFO	Population size	30
	Total iteration number	50
QIO	Population size	30
	Total iteration number	50
KMA	Population size	30
	Total iteration number	50
	Mlipir rate	0.5
	Female mutation rate	0.5
	Female mutation radius	0.5
GEO	Population size	30
	Total iteration number	50
	Propensity to attack	$[0.5,\ 2]$
	Propensity to cruise	$[1,\ 0.5]$
SMA	Population size	30
	Total iteration number	50
	Control parameter z	0.03

Table 4. Parameters settings of the adopted algorithms.

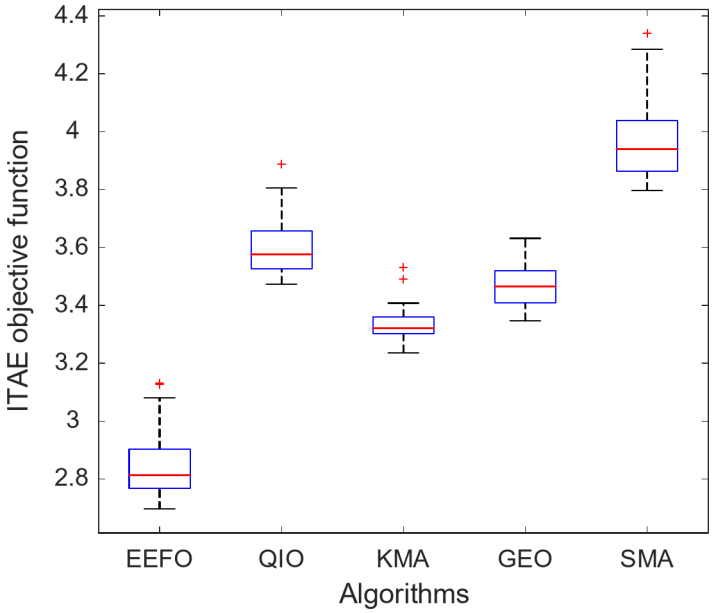


Fig. 4. Boxplot analysis.

Algorithm	Minimum	Maximum	Average	Standard Deviation	Friedman's mean rank
EEFO	2.6957	3.1310	2.8479	0.1199	1
QIO	3.4737	3.8874	3.6065	0.1048	4
KMA	3.2355	3.5315	3.3356	0.0678	2
GEO	3.3463	3.6314	3.4675	0.0726	3
SMA	3.7972	4.3394	3.9689	0.1485	5

Table 5. Statistical results obtained from different algorithms.

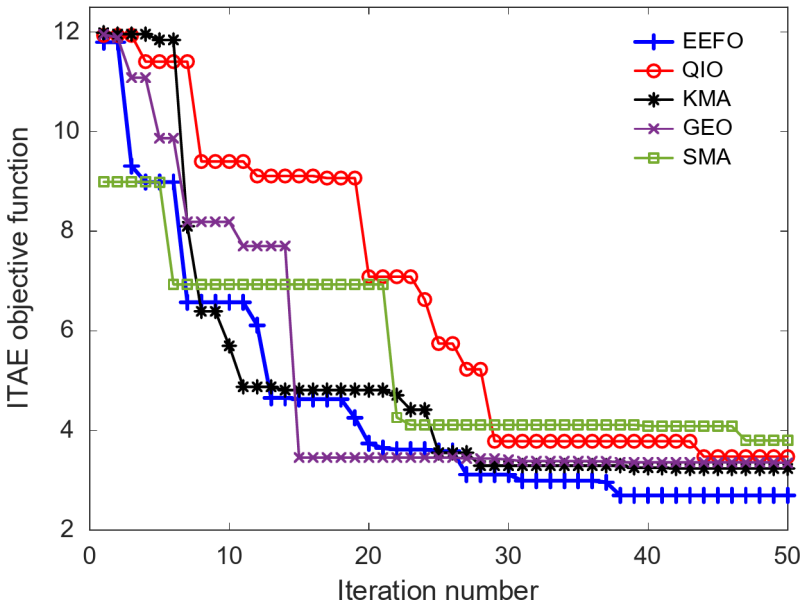


Fig. 5. Convergence curves for ITAE objective function obtained from different algorithms.

Algorithm	K_{p1}	K_i	K_{p2}	K_d	N
EEFO	15.0267	0.3086	4.8033	2.5105	198.0022
QIO	18.0291	0.5030	3.0402	1.5102	159.2288
KMA	18.3528	0.3934	4.0874	1.9076	258.4675
GEO	10.6192	0.5043	2.8962	1.5932	344.9394
SMA	16.7743	0.4045	4.0453	1.8476	209.6003

Table 6. Obtained controller parameters via different algorithms.

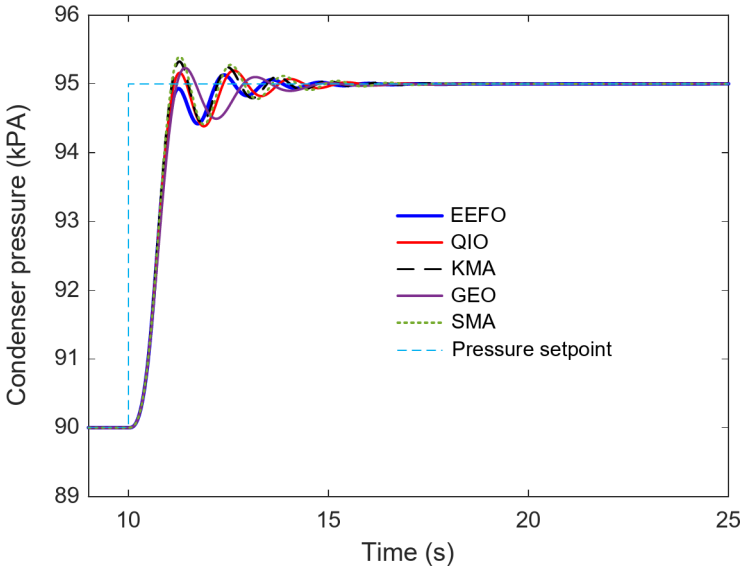


Fig. 6. Time response of the condenser pressure via different algorithms.

SMA, indicates a more controlled approach to managing system noise, ensuring stability without dampening the response. The overall combination achieved by EEFO results in a more robust and stable control performance, leading to lower ITAE values.

The time response of the condenser pressure under the control of different algorithms is compared in Fig. 6, and Fig. 7 provides a closer examination of the time response during critical periods. Although, the rise time is similar across all methods, the EEFO-based controller excels in minimizing settling time, overshoot, and steady-state error. This indicates that the EEFO-optimized controller not only achieves a fast response but also ensures stability and precision, which are crucial in maintaining the desired pressure levels in the steam condenser without causing undue stress on the system. This level of control is particularly important in industrial applications where precise regulation of process variables is necessary to avoid damaging equipment and ensure consistent product quality.

Table 7 compares the normalized time response metrics across the different algorithms. The comparative statistical values in Table 7 highlight the effectiveness of the EEFO-based PI-PDN controller in terms of settling time, overshoot, ITAE, and steady-state error. Among all the tested optimization algorithms, EEFO achieves the lowest values in all performance metrics, demonstrating its superior ability to regulate condenser pressure efficiently. EEFO achieves the shortest normalized settling time (13.1799 s), indicating that the system stabilizes faster compared to other approaches. Faster stabilization is crucial in industrial processes where delays in control response can lead to inefficiencies and increased operational costs. The overshoot percentage (2.5609%) observed in EEFO-based control is significantly lower than the other algorithms. High overshoot values, as seen in SMA (7.9315%) and KMA (6.4680%), may introduce undesired fluctuations in the system, which can cause instability in real-world condenser pressure control applications. The ITAE value of 2.6957 further supports EEFO's robustness in reducing long-term deviations from the desired pressure setpoint. A lower ITAE value indicates that the EEFO-tuned controller provides smoother error minimization over time, avoiding sustained deviations from the target pressure. The steady-state error of EEFO (5.7304E − 07 kPa) is orders of magnitude lower than those obtained from QIO, KMA, GEO, and SMA. This minimal error confirms that the EEFO-based PI-PDN controller successfully maintains the target pressure over long operational periods, which is a crucial requirement for steam condensers. Overall, these results demonstrate that the EEFO-based PI-PDN controller effectively balances fast response and precision, making it more suitable for industrial applications compared to other optimization techniques.

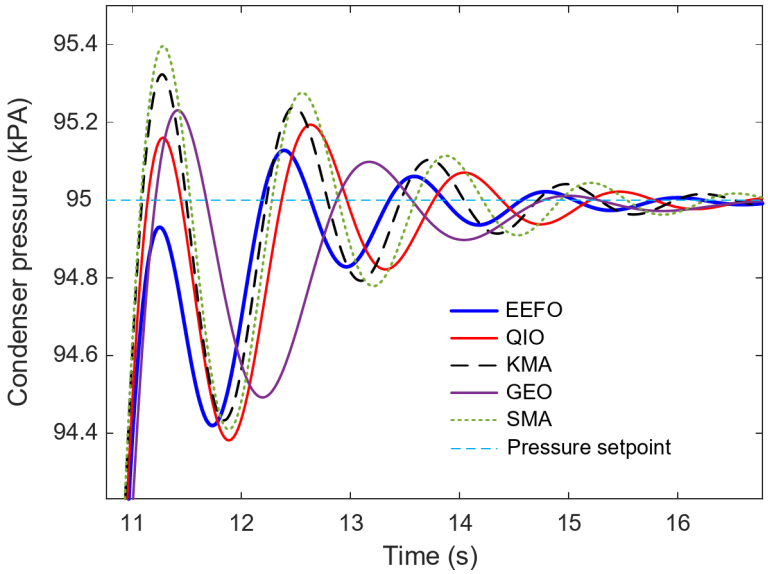


Fig. 7. Zoomed view of Fig. 6.

Algorithm	Normalized settling time (s)	Normalized overshoot (%)	$ITAE$ ($t_{fault} = 10$ s and $t_{sim} = 50$ s)	Steady-state error (kPA)
EEFO	13.1799	2.5609	2.6957	5.7304E − 07
QIO	13.5744	3.8836	3.4737	4.7256E − 04
KMA	13.7774	6.4680	3.2355	2.4718E − 04
GEO	14.1196	4.6208	3.3463	1.6505E − 04
SMA	13.9776	7.9315	3.7972	5.3114E − 04

Table 7. Normalized time response metrics obtained via different algorithms.

Comparisons with documented studies

The effectiveness of the EEFO-based PI-PDN controller was further validated through comparisons with documented studies involving other control strategies, including CSA-based FOPID [8], RIME-based FOPID [9], GWO-based PI [10], and GA-based PI [12]. The time response of the condenser under the EEFO-based PI-PDN controller with those documented in previous studies is compared as can be seen in Fig. 8. The EEFO-based controller achieves faster and more stable responses compared to the other methods, demonstrating its ability to handle the nonlinear dynamics of the steam condenser more effectively.

Figure 9 offers a closer look at the comparative time responses during critical transitions. The EEFO-based control strategy clearly outperforms the others in maintaining stability and minimizing transient deviations, which are essential for ensuring the safe and efficient operation of the steam condenser.

Comparative normalized time response metrics using documented studies are provided in Table 8. The comparison in Table 8 illustrates the significant advantages of the proposed EEFO-based PI-PDN controller over existing documented studies, which include CSA-based FOPID, RIME-based FOPID, GWO-based PI, and GA-based PI. The EEFO-based PI-PDN controller achieves a normalized settling time of 13.1799 s, which is notably lower than the 17.0509 s observed in CSA-based FOPID and 28.2457 s in GA-based PI. This indicates that the EEFO-tuned controller ensures a faster return to steady-state conditions after disturbances, significantly improving system responsiveness. The overshoot percentage of the EEFO-based controller (2.5609%) is considerably lower than the values obtained using CSA-based FOPID (12.0526%) and RIME-based FOPID (17.7156%). This reduced overshoot means that EEFO prevents excessive pressure deviations that could potentially damage condenser components or disrupt thermal plant operations. The ITAE value (2.6957) in EEFO-based PI-PDN control is significantly lower than that of CSA-based FOPID (14.3100) and RIME-based FOPID (15.9775), confirming its ability to minimize cumulative errors over time. This is a crucial indicator of the controller's efficiency in maintaining long-term stability. The EEFO-based controller's steady-state error (5.7304E − 07 kPa) is drastically lower than those found in previous studies, especially when compared to CSA-based FOPID (6.5730E − 04 kPa) and GA-based PI (0.0059 kPa). These results suggest that EEFO provides a superior long-term pressure regulation strategy, ensuring consistent system performance with minimal deviations. Overall, these findings validate that EEFO is a highly effective tool for optimizing nonlinear condenser pressure control, outperforming both classical and modern optimization techniques in achieving better stability, faster settling times, lower overshoot, and reduced steady-state error. The superior performance

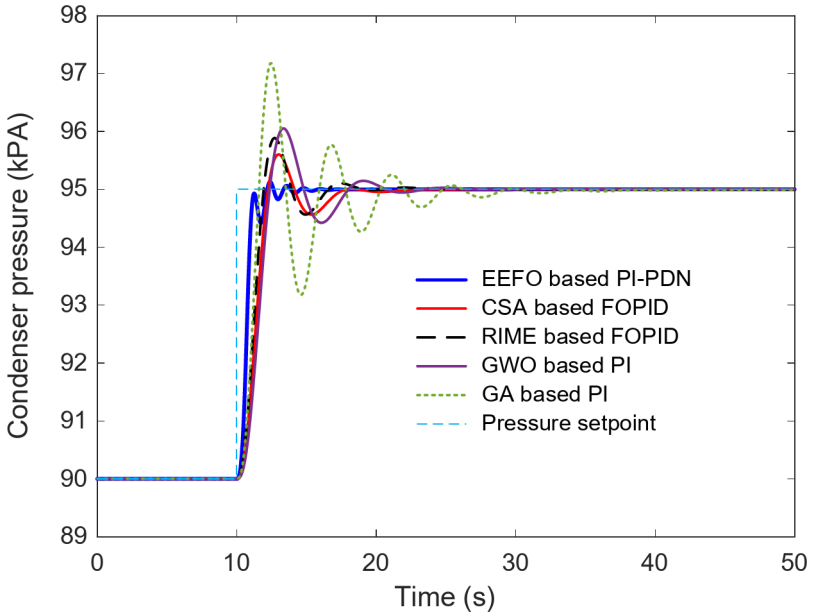


Fig. 8. Comparative time response of the condenser with the documented studies.

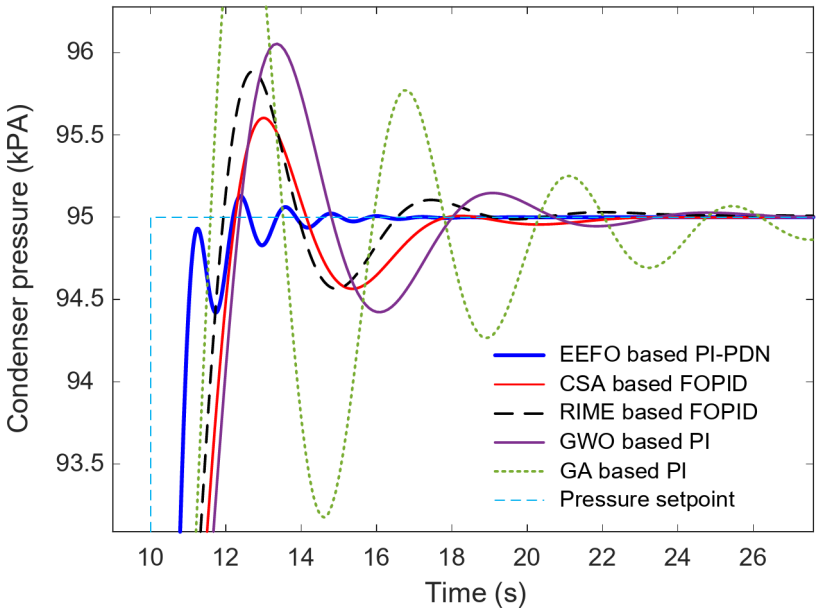


Fig. 9. Zoomed view of Fig. 8.

Control method	Normalized settling time (s)	Normalized overshoot (%)	$ITAE$ ($t_{fault} = 10$ s and $t_{sim} = 50$ s)	Steady-state error (kPA)
EEFO based PI-PDN (proposed)	13.1799	2.5609	2.6957	5.7304E − 07
CSA based FOPID[8]	17.0509	12.0526	14.3100	6.5730E − 04
RIME based FOPID[8]	17.6610	17.7156	15.9775	0.0053
GWO based PI[12]	19.8228	21.0680	23.8138	1.0680E − 04
GA based PI[12]	28.2457	43.5800	64.5673	0.0059

Table 8. Comparative normalized time response metrics using documented studies.

of EEFO in both metaheuristic algorithm comparisons and documented studies highlights its potential for broader industrial applications where precise and robust control is required.

Tracking input signal

Accurate tracking of input signals is crucial for maintaining optimal system performance, especially in dynamic environments. The ability of the EEFO-based PI-PDN controller to track input signals accurately is illustrated in Fig. 10. The results demonstrate that the proposed control strategy maintains close adherence to the desired input trajectory, ensuring that the system responds effectively to changes in operating conditions. This capability is vital for maintaining process stability and achieving the desired outcomes in real-time applications.

Effect of non-ideal conditions on proposed EEFO based PI-PDN controller performance

To assess the robustness of the proposed control strategy, the performance of the EEFO-based PI-PDN controller was evaluated under non-ideal conditions, including the presence of external disturbances and random noise. The external disturbance signal ($D(s)$) and noise signal ($N(s)$) were introduced to the system to simulate real-world operating conditions that can affect the stability and accuracy of the control process. The $D(s)$ represents external forces or influences that may alter the system's behavior, while the noise signal $N(s)$ is modeled as a uniformly distributed random noise within the range of $[-0.01,\ 0.01]$ kPA, with a sample time of 0.1 s. These noise and disturbance signals were applied to test the controller's ability to maintain stability and accurate pressure control despite these perturbations. Additionally, saturation limits were set between $[-50,\ 50]$ to simulate the physical constraints of the actuator, ensuring that the control actions remain within feasible operational bounds. The design of the control system, detailing how the external disturbance $D(s)$ and noise signal $N(s)$ were integrated into the simulation environment is illustrated in Fig. 11. The inclusion of these factors ensures a realistic assessment of the controller's performance under challenging conditions.

Figure 12 demonstrates that the EEFO-based controller effectively mitigates the impact of both noise and disturbances, maintaining stable and precise control of the condenser pressure. Despite the presence of random noise and external disturbances, the controller successfully keeps the system within the desired operating parameters, illustrating its robustness and reliability. The ability to handle such non-ideal conditions without significant degradation in performance is critical for industrial applications where external factors are often unpredictable and unavoidable.

5.5. Closed-loop response of the proposed control strategy

The closed-loop response of the proposed control strategy was analyzed to ensure that the controller performs effectively under varying operational conditions, including changes in circulating water outlet temperature, cooling water flow, and steam heat. Figure 13 illustrates the closed-loop response, confirming that the EEFO-based PI-PDN controller maintains system stability and achieves the desired control objectives under dynamic conditions. The ability to adapt to changes in key process variables without sacrificing control quality is crucial for ensuring the long-term reliability and efficiency of the steam condenser system. A comprehensive analysis of the simulation results, demonstrating the superior performance of the proposed EEFO-based cascaded PI-PDN controller has been provided. The detailed discussion highlights the advantages of EEFO in optimizing the nonlinear steam condenser system and confirms its robustness across various scenarios, including comparisons with recent metaheuristic algorithms, documented studies, and under non-ideal operating conditions. The findings validate the potential of EEFO as an advanced optimization tool for industrial control systems.

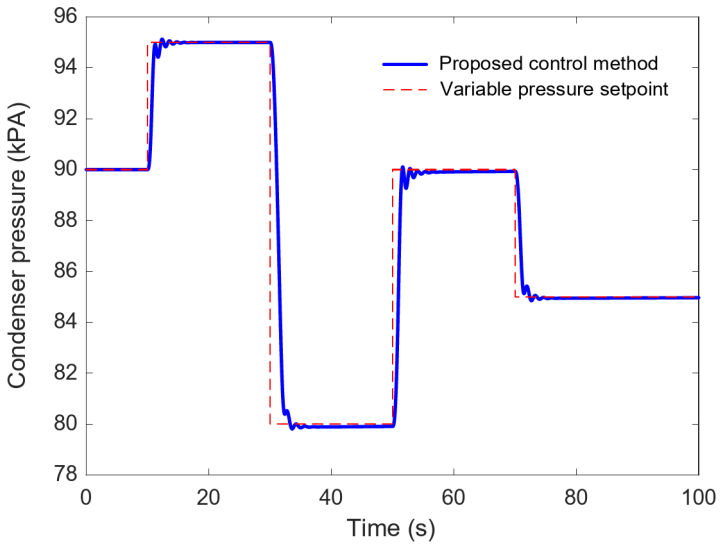


Fig. 10. Performance of the proposed control strategy in terms of input signal tracking.

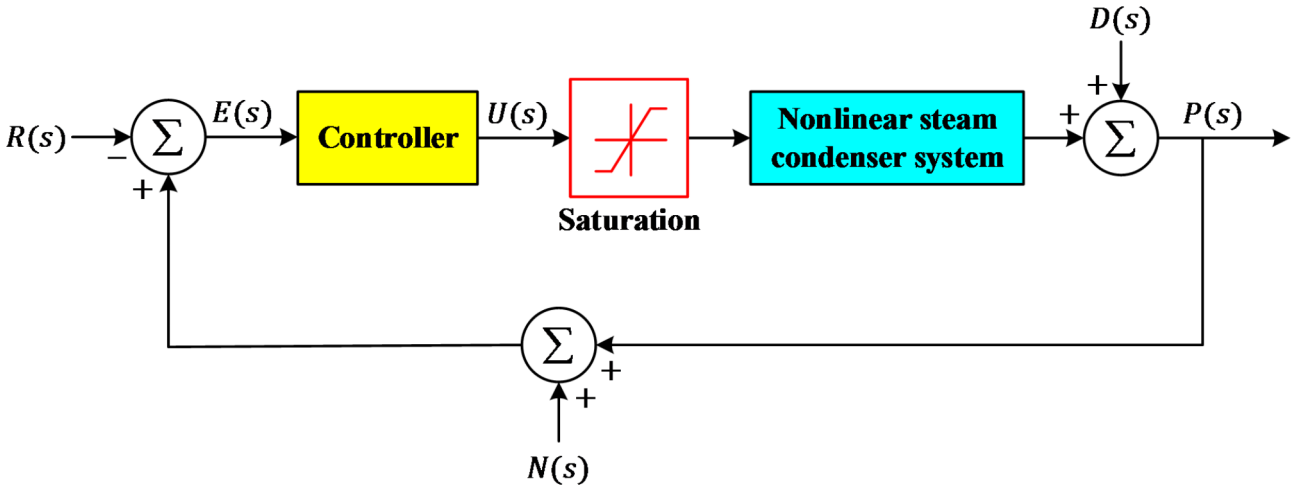


Fig. 11. Design of the proposed control system for saturation and disturbances.

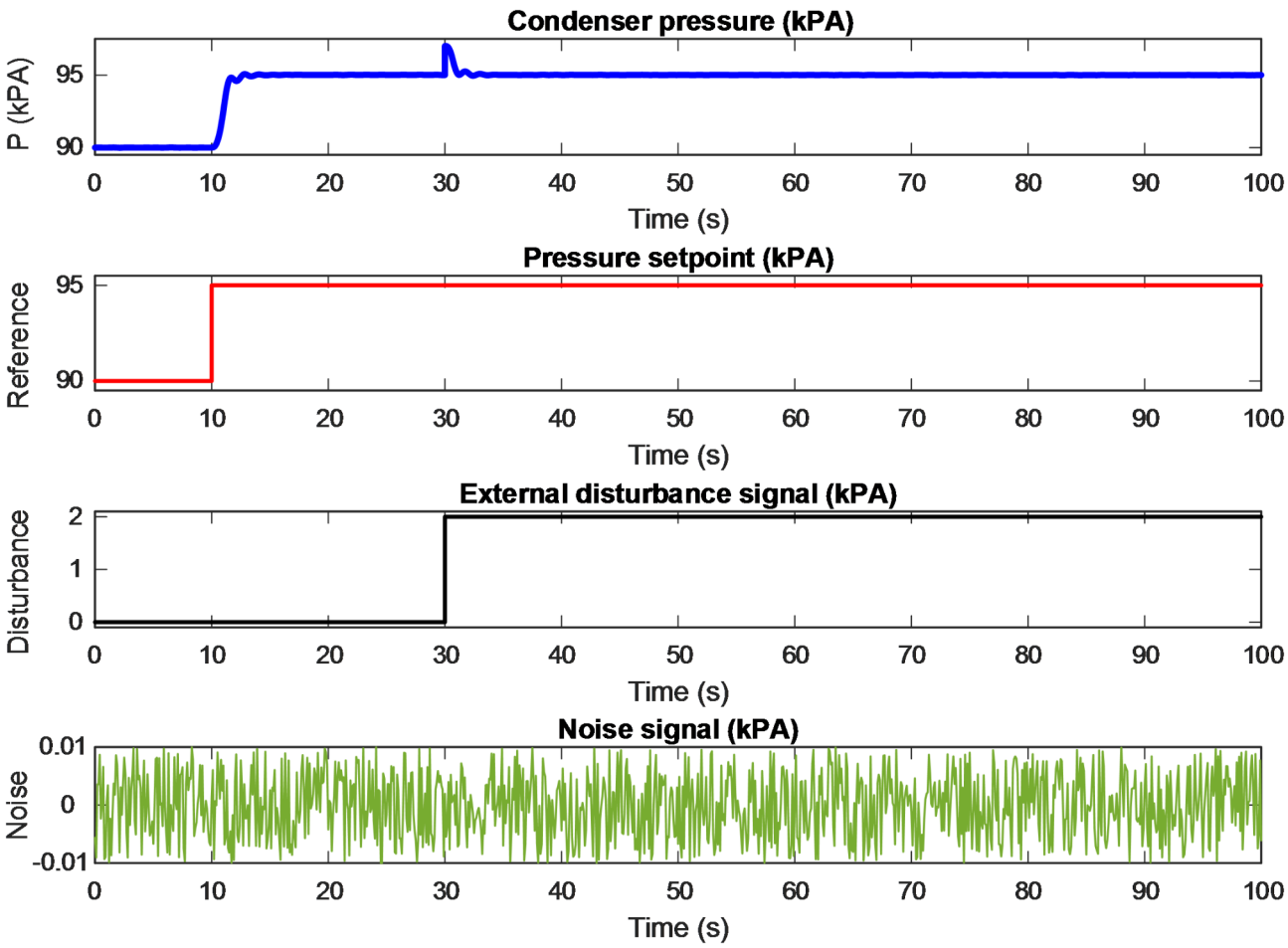


Fig. 12. Performance of the proposed control approach with respect to noise and disturbance effects.

6. Conclusion

In this study, it is proposed a novel approach to optimizing the control of a nonlinear shell-and-tube steam condenser system using the EEFO. The cascaded PI-PDN controller, optimized through the EEFO algorithm, was designed to address the inherent challenges posed by system nonlinearities, external disturbances, and the complexity of tuning multiple control parameters in thermal power plant operations. The effectiveness of

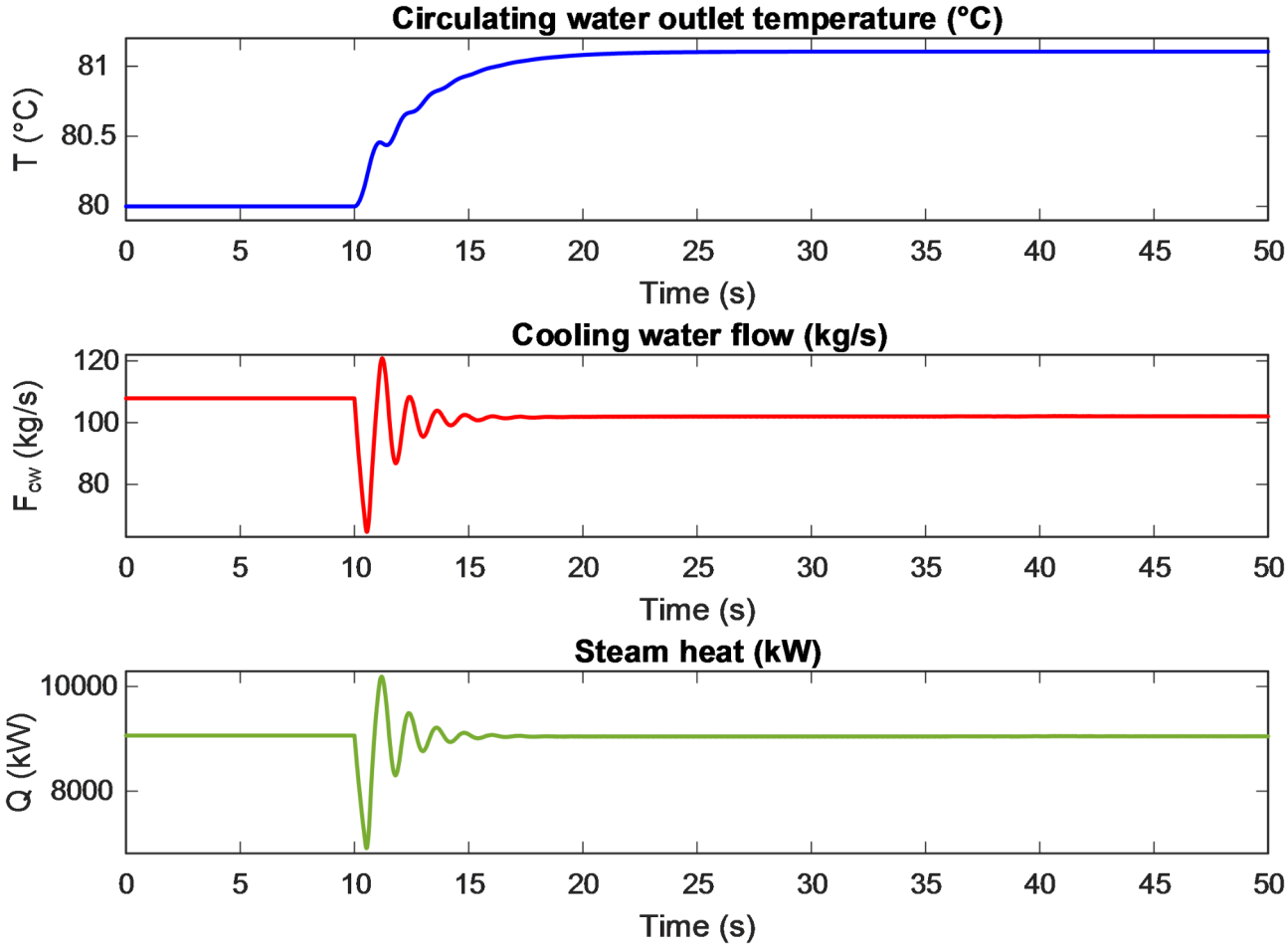


Fig. 13. Closed loop response of the proposed control strategy with respect to circulating water outlet temperature, cooling water flow and steam heat.

the EEFO-based cascaded PI-PDN controller control strategy was validated through extensive simulations and comparisons with several recent metaheuristic algorithms, including the SMA, GEO, KMA, and QIO. In addition, the proposed controller was further confirmed by comparing it with documented studies that utilized other control strategies, such as CSA-based FOPID, RIME-based FOPID, GWO-based PI, and GA-based PI. The simulation results demonstrated that the EEFO algorithm outperformed these algorithms in optimizing the ITAE objective function, achieving superior control performance across various metrics. Specifically, the EEFO-based PI-PDN controller exhibited enhanced system stability, reduced settling time, minimized overshoot, and lower steady-state error compared to the alternative methods. Furthermore, the robustness of the proposed control strategy was assessed under non-ideal conditions, including the presence of external disturbances and noise. The EEFO-based controller maintained its superior performance, demonstrating resilience in the face of operational challenges that typically degrade system performance. The comparative analysis with documented studies further underscored the advantages of the EEFO algorithm in this domain, as it consistently outperformed other established control strategies. The findings of this study quantitatively demonstrate that the EEFO-based PI-PDN controller outperforms existing optimization techniques and documented control strategies for steam condenser pressure regulation. Specifically, EEFO reduces settling time by 22.7%, overshoot by 78.7%, steady-state error by three orders of magnitude, and ITAE by 81.2% compared to metaheuristic based methods. These improvements highlight the effectiveness of EEFO in achieving faster convergence, better stability, and precise tracking performance, making it a viable solution for real-world industrial applications.

For future research, experimental validation of the proposed approach on a physical steam condenser setup would further strengthen its applicability in practical scenarios. Additionally, exploring hybrid optimization techniques, integrating EEFO with other bio-inspired algorithms, could further enhance convergence speed and robustness[35,36]. Investigating adaptive control frameworks, where the controller dynamically adjusts its parameters in real-time, could also improve performance under varying operating conditions[37]. Expanding this approach to multi-variable industrial processes, such as boiler pressure control and thermal energy storage systems, represents another promising avenue for future research. Lastly, the researchers may investigate the stability and sensitivity analyses in greater depth, ensuring its adaptability to real-world applications.

Data availability

The datasets used and/or analyzed during the current study available from the corresponding author on reasonable request.

Received: 10 September 2024; Accepted: 28 February 2025
Published online: 04 March 2025

References

1. Brodov, Y. M., Aronson, K. E., Ryabchikov, A. Y. & Nirenshteyn, M. A. Current state and trends in the design and operation of Water-Cooled condensers of steam turbines for thermal and nuclear power stations (Review). *Therm. Eng.* **66**, 16–26 (2019).
2. Pernica, M. et al. Transient thermal stress calculation of a shell and tube condenser with fixed tubesheet. *Chem. Ing. Tech.* **93**, 1590–1597 (2021).
3. Rifaldo, Z., Hafid, B., Husin, Z. & Idris, M. Etanto Heiliano Wijayanto Analysis of Heat Transfer in Shell and Tube Type Condensers. *Journal of Mechanical Engineering Manufactures Materials and Energy* **8**, 67–74 (2024).
4. Rakhimov, G. B. & Murtazayev, F. I. Increasing the efficiency of heat exchange by changing the construction of a shell-and-tube heat exchanger. *E3S Web of Conferences* 443, 03008 (2023).
5. Ekinci, S. et al. Optimizing steam condenser efficiency: integrating logarithmic spiral search and greedy selection mechanisms in gazelle optimizer for PI controller tuning. *Results Eng.* **24**, 103501 (2024).
6. Pereira, I. P. S., Bagajewicz, M. J. & Costa, A. L. H. Global optimization of the design of horizontal shell and tube condensers. *Chem. Eng. Sci.* **236**, 116474 (2021).
7. Rizk-Allah, R. M., Hassanien, A. E. & Marafie, A. An improved equilibrium optimizer for numerical optimization: A case study on engineering design of the shell and tube heat exchanger. *J. Eng. Res.* **12**, 240–255 (2024).
8. Alzakari, S. A., Izci, D., Ekinci, S., Alhussan, A. A. & Hashim, F. A. Nonlinear FOPID controller design for pressure regulation of steam condenser via improved metaheuristic algorithm. *PLoS One*. **19**, e0309211 (2024).
9. Spooner, J. T., Maggiore, M., Ordóñez, R. & Passino, K. M. *Stable Adaptive Control and Estimation for Nonlinear Systems* (Wiley, 2002). https://doi.org/10.1002/0471221139
10. Girirajan, B. & Rathikarani, D. Optimal CRONE controller using meta-heuristic optimization algorithm for shell and tube heat exchanger. *IOP Conf. Ser. Mater. Sci. Eng.* **1166**, 012058 (2021).
11. Salim, H., Faisal, K. & Jawad, R. Enhancement of Performance for Steam Turbine in Thermal Power Plants Using Artificial Neural Network and Electric Circuit Design. *Applied Computational Intelligence and Soft Computing* 1–9 (2018). (2018).
12. Li, S. X. & Wang, J. S. Dynamic modeling of steam condenser and design of PI controller based on grey Wolf optimizer. *Math. Probl. Eng.* **2015**, 1–9 (2015).
13. Malik, H., Ahmad, S. M. & Wadood, F. G. A. Optimized PI-PDN robust control of a 1-DOF Maglev precision position system. *IEEE Access.* **11**, 130955–130973 (2023).
14. Ziegler, J. G. & Nichols, N. B. Optimum settings for automatic controllers. *J. Fluids Eng.* **64**, 759–765 (1942).
15. Izci, D., Ekinci, S., Eker, E. & Abualigah, L. Opposition-Based Arithmetic Optimization Algorithm with Varying Acceleration Coefficient for Function Optimization and Control of FES System. in *Proceedings of International Joint Conference on Advances in Computational Intelligence* (eds. Uddin, M. S., Jamwal, P. K. & Bansal, J. C.) 283–293 (Springer Singapore, 2022). https://doi.org/10.1007/978-981-19-0332-8_20
16. Cohen, G. H. & Coon, G. A. Theoretical consideration of retarded control. *J. Fluids Eng.* **75**, 827–834 (1953).
17. Shaukat, N., Khan, B., Ali, S. M., Munawar, U. & Ullah, Z. Comparative study of control methods for steam condenser. in *International Conference on Energy Conservation and Efficiency (ICECE)* 32–37 (IEEE, 2017). (2017). https://doi.org/10.1109/ECE.2017.8248825
18. Han, S. et al. Thermal-economic optimization design of shell and tube heat exchanger using an improved sparrow search algorithm. *Therm. Sci. Eng. Progress*. **45**, 102085 (2023).
19. Li, S., Chen, H., Wang, M., Heidari, A. A. & Mirjalili, S. Slime mould algorithm: A new method for stochastic optimization. *Future Generation Comput. Syst.* **111**, 300–323 (2020).
20. Mohammadi-Balani, A., Dehghan Nayeri, M., Azar, A. & Taghizadeh-Yazdi, M. Golden eagle optimizer: A nature-inspired metaheuristic algorithm. *Comput. Ind. Eng.* **152**, 107050 (2021).
21. Suyanto, S., Ariyanto, A. A. & Ariyanto, A. F. Komodo Mlipir algorithm. *Appl. Soft Comput.* **114**, 108043 (2022).
22. Zhao, W. et al. Quadratic interpolation optimization (QIO): A new optimization algorithm based on generalized quadratic interpolation and its applications to real-world engineering problems. *Comput. Methods Appl. Mech. Eng.* **417**, 116446 (2023).
23. Turgut, M. S., Turgut, O. E. & Abualigah, L. Chaotic quasi-oppositional arithmetic optimization algorithm for thermo-economic design of a shell and tube condenser running with different refrigerant mixture pairs. *Neural Comput. Appl.* **34**, 8103–8135 (2022).
24. Saari, J. et al. Techno-economic optimization of a district heat condenser in a small cogeneration plant with a novel greedy cuckoo search. *Energy* **239**, 122622 (2022).
25. Izci, D., Ekinci, S., Abualigah, L., Salman, M. & Rashdan, M. Parameter extraction of photovoltaic cell models using electric eel foraging optimizer. *Front. Energy Res.* **12**, 1407125 (2024).
26. Abdelwahab, S. A. M. et al. Optimal control and optimization of Grid-Connected PV and wind turbine hybrid systems using electric eel foraging optimization algorithms. *Sensors* **24**, 2354 (2024).
27. Alzakari, S. A., Izci, D., Ekinci, S., Alhussan, A. A. & Hashim, F. A. A new control scheme for temperature adjustment of electric furnaces using a novel modified electric eel foraging optimizer. *AIMS Math.* **9**, 13410–13438 (2024).
28. Zhao, W. et al. Electric eel foraging optimization: A new bio-inspired optimizer for engineering applications. *Expert Syst. Appl.* **238**, 122200 (2024).
29. Mehta, P., Yildiz, B. S., Sait, S. M. & Yıldız, A. R. Optimization of electric vehicle design problems using improved electric eel foraging optimization algorithm. *Mater. Test.* **66**, 1230–1240 (2024).
30. Al-qaness, M. A. A. et al. Optimized quantum LSTM using modified electric eel foraging optimization for real-world intelligence engineering systems. *Ain Shams Eng. J.* **15**, 102982 (2024).
31. Jabari, M. et al. Efficient pressure regulation in nonlinear shell-and-tube steam condensers via a novel TDn(1 + PIDn) controller and DCSA algorithm. *Sci. Rep.* **15**, 2090 (2025).
32. Izci, D., Köse, E., Ekinci, S. & Feedforward-Compensated, P. I. Controller design for Air–Fuel ratio system control using enhanced weighted mean of vectors algorithm. *Arab. J. Sci. Eng.* **48**, 12205–12217 (2023).
33. Ekinci, S., Izci, D., Can, O., Bajaj, M. & Blazek, V. Frequency regulation of PV-reheat thermal power system via a novel hybrid educational competition optimizer with pattern search and cascaded PDN-PI controller. *Results Eng.* **24**, 102958 (2024).
34. Ekinci, S., Izci, D., Ghandour, R., Salman, M. & Turkeri, C. Aquila Optimizer-Based Filtered PID Controller Design for A Spark Ignition Engine Speed Control. in *2024 8th International Symposium on Innovative Approaches in Smart Technologies (ISAS)* 1–5IEEE, (2024). https://doi.org/10.1109/ISAS64331.2024.10845268
35. Nayak, P. C., Mishra, S., Prusty, R. C. & Panda, S. Hybrid Whale optimization algorithm with simulated annealing for load frequency controller design of hybrid power system. *Soft Comput.* https://doi.org/10.1007/s00500-023-09072-1 (2023).

36. Nayak, P. C., Prusty, R. C. & Panda, S. Adaptive fuzzy approach for load frequency control using hybrid moth flame pattern search optimization with real time validation. *Evol. Intell.* **17**, 1111–1126 (2024).
37. Mishra, D., Nayak, P. C., Prusty, R. C. & Panda, S. An improved equilibrium optimization-based fuzzy Tilted double integral derivative with filter (F-TIDF-2) controller for frequency regulation of an off-grid microgrid. *Electr. Eng.* **106**, 2033–2055 (2024).

Acknowledgements
This research is funded by European Union under the REFRESH—Research Excellence For Region Sustainability and High-Tech Industries Project via the Operational Programme Just Transition under Grant CZ.10.03.01/00/22_003/0000048; in part by the National Centre for Energy II and ExPEDite Project a Research and Innovation Action to Support the Implementation of the Climate Neutral and Smart Cities Mission Project TN02000025; and in part by ExPEDite through European Union's Horizon Mission Programme under Grant 101139527. The authors would like to express their sincere gratitude to Stanislav Misak for his exceptional supervision, project administration, and overall guidance throughout the course of this project. His expertise and support were instrumental to its success.

Author contributions
Serdar Ekinci, Cebrail Turkeri: Conceptualization, Methodology, Software, Visualization, Investigation, Writing- Original draft preparation. Davut Izci, Laith Abualigah: Data curation, Validation, Supervision, Resources, Writing - Review & Editing. Mohit Bajaj, Vojtech Blazek, Lukas Prokop: Project administration, Supervision, Resources, Writing - Review & Editing.

Declarations

Competing interests
The authors declare no competing interests.

Additional information
Correspondence and requests for materials should be addressed to M.B.

Reprints and permissions information is available at www.nature.com/reprints.

Publisher's note Springer Nature remains neutral with regard to jurisdictional claims in published maps and institutional affiliations.

Open Access This article is licensed under a Creative Commons Attribution-NonCommercial-NoDerivatives 4.0 International License, which permits any non-commercial use, sharing, distribution and reproduction in any medium or format, as long as you give appropriate credit to the original author(s) and the source, provide a link to the Creative Commons licence, and indicate if you modified the licensed material. You do not have permission under this licence to share adapted material derived from this article or parts of it. The images or other third party material in this article are included in the article's Creative Commons licence, unless indicated otherwise in a credit line to the material. If material is not included in the article's Creative Commons licence and your intended use is not permitted by statutory regulation or exceeds the permitted use, you will need to obtain permission directly from the copyright holder. To view a copy of this licence, visit http://creativecommons.org/licenses/by-nc-nd/4.0/.

© The Author(s) 2025